



Deposited via The University of Leeds.

White Rose Research Online URL for this paper:

<https://eprints.whiterose.ac.uk/id/eprint/199574/>

Version: Accepted Version

Article:

Yu, K, Chen, L, Zhang, W et al. (2023) Behaviour of polymer-coated composite nanoparticles at bubble-stabilizing interfaces during bubble coarsening and accelerated coalescence: A Cryo-SEM study. *Journal of Colloid and Interface Science*, 633. pp. 113-119. ISSN: 0021-9797

<https://doi.org/10.1016/j.jcis.2022.11.100>

© 2022, Elsevier. This manuscript version is made available under the CC-BY-NC-ND 4.0 license <http://creativecommons.org/licenses/by-nc-nd/4.0/>.

Reuse

This article is distributed under the terms of the Creative Commons Attribution-NonCommercial-NoDerivs (CC BY-NC-ND) licence. This licence only allows you to download this work and share it with others as long as you credit the authors, but you can't change the article in any way or use it commercially. More information and the full terms of the licence here: <https://creativecommons.org/licenses/>

Takedown

If you consider content in White Rose Research Online to be in breach of UK law, please notify us by emailing eprints@whiterose.ac.uk including the URL of the record and the reason for the withdrawal request.

Behaviour of polymer-coated composite nanoparticles at bubble-stabilizing interfaces during bubble coarsening and accelerated coalescence: A Cryo-SEM study

Kai Yu^{1*}, Liuha Chen¹, Weifeng Zhang¹, Huagui Zhang², Jianguang Jia¹, Zhentao Wang¹, Bin Li^{1*}, Wei Zhang¹, Haojie Xu¹, Lei Zuo¹, Junfeng Wang¹, Jianming Pan³, David Harbottle⁴

¹ School of Energy and Power Engineering, Jiangsu University, Zhenjiang 212013, China

² College of Chemistry and Materials Science, Fujian Key Laboratory of Polymer Science, Fujian Normal University, Fuzhou 350007, China

³ School of Chemistry and Chemical Engineering, Jiangsu University, Zhenjiang, 212013, China

⁴ School of Chemical and Process Engineering, University of Leeds, Leeds, U.K.

ABSTRACT

Hypothesis: Dynamics of polymer-coated silica composite nanoparticles (CPs) during bubble coarsening is highly dominated by the behaviour of the polymer layer, while *in-situ* particle aggregation would lead to accelerated bubble coalescence.

Experiments: CPs-stabilized foams were prepared in 0.1 M and 0.55 M Na₂SO₄ solution, referring to the 0.1 M and 0.55 M foam/bubble respectively. The 0.1 M to 0.55 M transition foam was also prepared. High resolution Cryo-SEM was originally used to investigate the CPs behaviour at the bubble-stabilizing interface during bubble coarsening and accelerated coalescence.

Findings: The 0.1 M bubble-stabilizing interface buckles in uniaxial compression due to coarsening, with the CPs being observed to desorb from the interface. While the CPs were visualized to rearrange into crumpled particle multi-layers surrounding the shrinking 0.55 M bubbles, due to the adhesion between interpenetrating polymer chains and the unique lubrication

effect of the PVP layers. The 0.1 M to 0.55 M transition foaming behaviour was also studied. Cracks and voids were observed at interfaces surrounding the transition bubbles driven by *in-situ* particle aggregation, resulting in accelerated bubble coalescence during the transition process.

Keywords: Polymer-coated particles; Cryo-SEM; Particle-laden interfaces; Particle rearrangement

1. INTRODUCTION

Smart foams and emulsions are finding more applications in biomedicine (e.g., controlled release), materials science (e.g., all-liquid materials and template for porous materials), agricultural science (e.g., pesticide spraying) and formulated products.[1-3] Contrary to classical surfactant-stabilised systems, particle-laden interfaces are typically not in global thermodynamic equilibrium and can be kinetically arrested, especially when interfaces are formed by mechanical forces and particles are trapped during formation.[4] The adsorption of particles at interfaces offers resistance against deformation coarsening and coalescence, and it is possible to kinetically arrest non-equilibrium constructs, resulting in vastly expanded design parameters.[5]

There is a good understanding of and available measurement techniques for the effects of particle size and three phase contact-angle controlling the adsorption energy. For instance, interfacial behaviour of particles has normally been studied at 2D planar interface, e.g., using interfacial shear rheometer and Langmuir trough.[6, 7] Research has found that coalescence of foams and emulsions is determined by the shear rheology of particle-laden interface, where bubble/droplet coalescence can be highly restrained once the interfaces become elastically dominant ($G' \gg G''$, where G' and G'' are the shear elastic and viscous moduli, respectively).[8] While bubble/droplet coarsening is usually linked to compression elasticity of the interface.[9] Furthermore, structure of the interfacial film is able to monitor *in-situ* using Brewster angle microscopy (BAM), with a resolution up to 2 μm . Whereas for any sub-micron structures, the Langmuir-Blodgett (LB) method can be used to recover the film from the interface, which can then be examined using SEM or TEM to get information of nanoscale structure.[4]

Particle shape, size, and surface chemistry (charge, wettability, patchiness) control foam/emulsions stability and properties and there is existing know-how on how to design particles with specific qualities.[10-14] Compared to hard particles, using deformable composite particles such as surfactant- and polymer-coated particle composites to stabilize interfaces provides additional tuning parameters, which can be triggered by temperature, pH, or light for example, to deliver function to foams and emulsions.[4, 10, 15] Composite particles are increasingly of interest because they lower surface/interfacial tensions and form strong protective viscoelastic barriers that inhibit coalescence of bubbles/droplets, with excellent viscoelasticity partly attributed to the particles ability to deform and interpenetrate neighbouring particles.[5, 7, 16-18] Recently, a novel kind of composite nanoparticles (CPs) was produced by coating silica nanoparticles with poly(vinylpyrrolidone) (PVP). Interfacial dynamics of the CPs indicated an ascendancy of the PVP-PVP interaction to regulate the viscoelasticity of CPs-stabilized films. Hence, the CPs-stabilized foam showed stimuli-responsive behaviour for different electrolyte concentrations, due to the alteration of PVP-PVP interaction.[19] More recently, we found that mobility of the CPs at interfaces is also strongly dominated by the compliance of the PVP layer. Therefore, changing PVP-shell-thickness of the CPs would also modulate interfacial dynamics of the CPs and the related foam stability.[5, 17] However, behaviour of the CPs at bubble-stabilizing interface (curved interface) during bubble coarsening and coalescence is still poorly understood.[20]

In the current study, to better understand the underlying bubble coarsening mechanism, high resolution Cryo-SEM was originally used to investigate the behaviour of CPs at the bubble-stabilizing interface during coarsening. Also revealed is the mechanism of accelerated bubble coalescence induced by *in-situ* particle aggregation.

2. MATERIALS AND METHODS

2.1 Materials. Silica nanoparticles (diameter of ~ 29.5 nm measured by SEM), PVP (MW of 40 kDa) and Na₂SO₄ were purchase from Sigma-Aldrich, Alfa Aesar and Sigma-Aldrich, respectively. Deionized water was utilized for all the tests presented in this work.

2.2 CPs preparation. The CPs were produced by decorating the silica nanoparticles with PVP via hydrogen bond, forming a core-shell structure.[21] The successful formation of the CPs was proved by TEM study (Fig. S1), where the silica particle-core and the PVP-shell can be clearly observed. Hydrodynamic diameter of the CPs were measured to be ~52 nm in Milli-Q water (Malvern Instruments, UK), with a hydrated PVP-shell thickness of ~9 nm.[21] It should note that the PVP-shell thickness would decrease with increasing electrolyte concentration, which will be discussed in more details below.

2.3 Interface characterization. Surface pressure–area ($\Pi - A$) isotherms were used to characterize compressibility of the interfacial CPs film, where the air-aqueous interface was built inside a Langmuir trough. Moreover, the interfacial CPs films were recovered by the LB method at different surface pressures, and the structure of which was imaged using the SEM. More details about the interface characterization can refer to Yu et al. [5, 17, 21]

2.4 Foam Studies. *2.4.1 Preparation of the 0.1 and 0.55 M foams.* The 0.1 M and 0.55 M foams/bubbles were generated by fierce handshaking of the CPs suspension (1 wt%) for one minute, where the Na₂SO₄ concentrations in the suspension were 0.1 M and 0.55 M, respectively. Height of the foams was measured over time to evaluate the foam stability. Meanwhile, foam coarsening was studied by sealing some foam samples inside flat-edged capillary tubes, while size of the bubbles was monitored over time using an optical microscope. More details on foam preparation and characterization, including the Cryo-SEM study, can be found in the Supporting Information and in Yu et al.[21]

2.4.2 Preparation of transition foams. The 0.1 M to 0.55 M transition foaming behavior was studied by generating foams at 0.1 M Na₂SO₄ followed by increasing the bulk electrolyte concentration to 0.55 M *in-situ*, as shown in Scheme S1 (Supporting Information). Injection of the additional Na₂SO₄ solution was carried out using a syringe with a long needle. The injection speed was carefully controlled to minimize the disturbance to the existing foams. The remained foams after injection was named the transition foams. The final electrolyte concentration and liquid

volume in the transition foam sample were 0.55 M and 10 ml, respectively. Height of the transition foams was measured over time to characterize the foam stability.

3. RESULTS AND DISCUSSION

3.1 Interfacial behaviour of CPs during bubble coarsening

3.1.1 Coarsening of the 0.1 M foam. The CPs were proved to be excellent foaming agents, with foam stability controlled by the electrolyte concentration (Na_2SO_4). [21] Using high resolution Cryo-SEM imaging, behaviour of the CPs at bubble-stabilizing interface was studied. Immediately after foaming, most of the bubbles in 0.1 M Na_2SO_4 (the 0.1 M bubbles) were measured to be 50-250 μm in size (Fig. S2). Fig. 1a shows a Cryo-SEM image of a CPs-stabilized bubble in the freshly prepared 0.1 M foam, while Fig. 1b shows high magnification Cryo-SEM images of the CPs-laden interface in Fig. 1a. The CPs were found to be closely-packed at the interface, approaching a $\sim 100\%$ apparent particle surface coverage (Fig. 1b), although a few black points were seen between the CPs, which may indicate some nanoscale vacancies in-between (see inset of Fig. 1b).

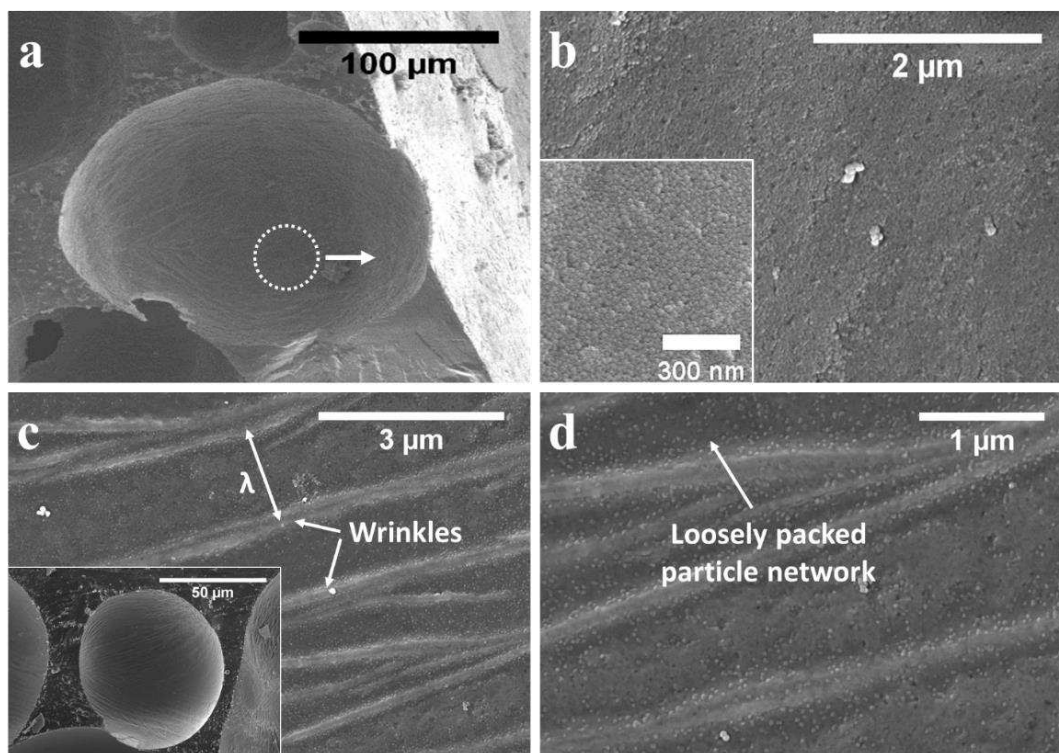


Figure 1. CPs-laden interfaces surrounding (a, b) newly-prepared and (c, d) aged air bubbles in 0.1 M Na₂SO₄. (b) Higher magnification image of the 0.1 M bubble-stabilizing interface in Fig. 1a, the inset shows a zoomed-in image. (d) Higher magnification image of the interface in Fig. 1c. An aged 0.1 M bubble is shown in Fig. 1c as an inset.

Behaviour of the CPs at a planar air-aqueous interface was also studied using a Langmuir trough (Fig. 2a). Surface pressure of the CPs layer increases upon compression, suggesting an increasingly compacted CPs network. The interfacial CPs films were recovered via the LB method at various surface pressures (detailed elsewhere[21]), and their structures were imaged using SEM. A porous CPs network was observed at 3 mN/m in Fig. 2b-1, before the CPs film being further densified at 4 mN/m, approaching a closely-packed particle monolayer (Fig. 2b-2). Further compression leads to extrusion of excess CPs from the particle monolayer, forming a patchy particle multilayer at 5 mN/m (Fig. 2b-3). If we compare the structure of CPs films that formed at curved (Fig. 1b) and planar (Fig. 2b) interfaces, it may indicate that surface pressure of the CPs-stabilized interface surrounding freshly-prepared 0.1 M bubbles is higher than 3 mN/m while below 5 mN/m.

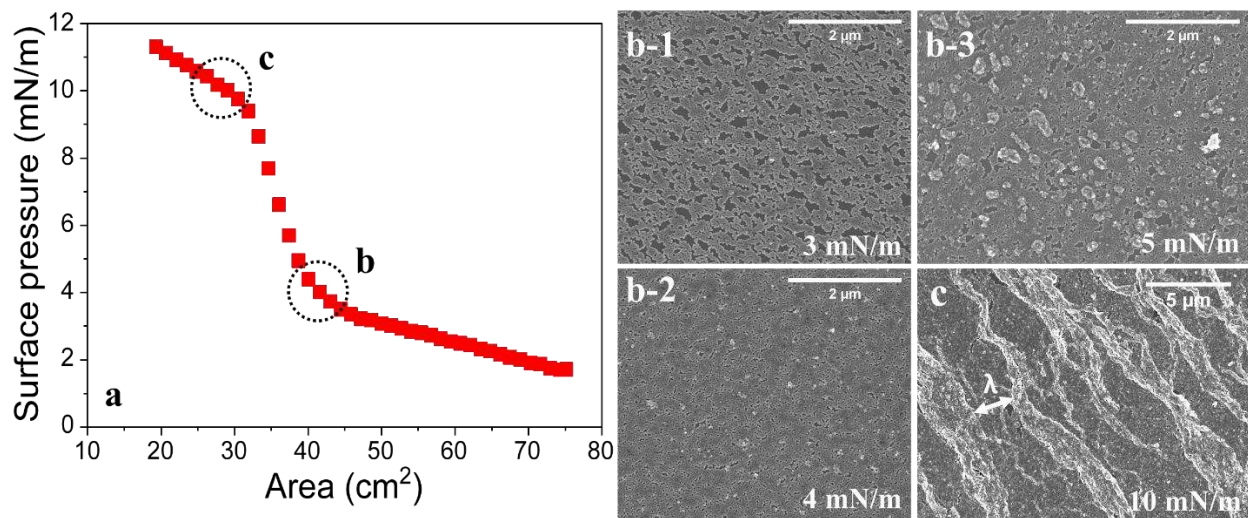


Figure 2. (a) $\Pi - A$ isotherms of CPs-laden interfaces at 0.1 M. (b, c) SEM images of 0.1 M CPs-stabilizing films recovered by LB method from a planar interface at $\Pi = 3, 4, 5$ and 10 mN/m, respectively.

The CPs films were found to be ‘pseudo-solid-like’ at 0.1 M Na₂SO₄, and neither bubble coarsening nor coalescence was inhibited in this condition.[21] The freshly prepared 0.1 M foams (Fig. S3a) were left undisturbed at room temperature for 0.5 hour, after which the aged foam samples were frozen for imaging by the Cryo-SEM. Fig. 1c and 1d show low and high magnification images of an aged 0.1 M bubble, on which substantial wrinkles were clearly observed. Those wrinkles suggests reduction of bubble surface area due to coarsening, leading to compression of the bubble-stabilizing film. The compressional behaviour of the 0.1 M CPs-laden planar interface was studied using a Langmuir trough, with similar crumpling CPs layers being observed when surface pressure > 9 mN/m (Fig. 2c).[21] Crumpling of the CPs-laden interface confirms its viscoelastic property, which also suggests that surface pressure of the 0.1 M bubble-stabilizing-film may be higher than 9 mN/m during bubble shrinking. Although bubble coarsening also leads to bubble expansion, bubble coarsening and coalescence take place simultaneously in this case, making it is difficult to identify the coarsening effect on bubble expanding. Hence, only shrinking bubbles were studied for the 0.1 M foam.

Individual particles can be clearly recognized in Fig. 1d, with diameter (d) of the CPs measured to be ~ 32.1 nm. While wrinkle wavelength (λ) of the interface surrounding bubbles was measured to be 1.7 ± 0.3 μm (Fig. 1c), in good agreement with that measured at planar interface (2.5 ± 0.7 μm) in Fig.2c. For particle-laden interfaces (air-liquid/liquid-liquid) under compression, the scaling relationship between the wrinkle wavelength and the particle diameter was reported to be: $\lambda \sim d^{0.5}$.[22] Insert our values ($d \approx 32.1 \times 10^{-9}$ m, $\lambda \approx 1.7 \times 10^{-6}$ m) into this relationship, yielding $\lambda \approx 0.01d^{0.5}$. Interestingly, unlike the densely packed CPs film surrounding fresh bubbles in Fig. 1b, vacancies of particle were observed in Fig. 1d for aged bubbles. Particle packing density at the interface tends to increase during bubble shrinking, until a critical point is met, where excess CPs would be extruded from the interface. Although the CPs were characterised to be hydrophilic (apparent contact angle < 90°),[4] no particle desorption was observed in the Langmuir trough study when the critical point was exceeded, in which case the excess CPs were extruded into the air phase, as being approved by Fig. 2b-3. However, it should be noted that particle extrusion also increases heterogeneity of the structure of the CPs-laden interface, since more and larger voids appear in Fig. 2b-3 ($\Pi = 5$ mN/m) compared with those in Fig. 2b-2 ($\Pi = 4$ mN/m). By contrast,

the CPs layers buckled towards the aqueous phase in a foam during bubble coarsening (Fig. 1c), making it much easier for the CPs to be extruded from the interface (to the aqueous phase) under compression, leading to particle desorption (Fig. 1d).

3.1.2 Coarsening of the 0.55 M foam. Aggregation of CPs became pronounced in 0.55 M electrolyte because of the adhesion between interpenetrating polymer chains (Fig. S1b). Adsorption of the fractal CPs aggregates at the interface upon foaming led to a porous structure as shown in Fig. 3a-b, with the apparent particle surface coverage measured to be ~ 95%. [23] Pore size of the interface was measured using a reported thresholding method by ImageJ (more than 1000 pores were considered) [23], suggesting that ~ 70% of the pore size is less than $0.2 \mu\text{m}^2$, whereas the other ~ 30% is in the range of $0.2 \mu\text{m}^2$ - $0.8 \mu\text{m}^2$ (inset of Fig. 3b). Structure of the 0.55 M bubble-stabilizing film was also studied via imaging from the inside of the bubbles, where voids were observed throughout the internal film of the 0.55 M bubble (Fig. 3c-d), further confirming the porous structure shown in Fig. 3a-b.

The CPs-laden interface became solid-like in 0.55 M Na_2SO_4 ($G' \gg G''$), and coarsening was recognized to be the predominant mechanism for foam collapse. [21] Smaller bubbles ($< 300 \mu\text{m}$ in size) shrinking while larger bubbles ($> 700 \mu\text{m}$ in size) expanding over time were observed due to coarsening. Although aggregation of the CPs at 0.55 M increases interface viscoelasticity, the PVP shells produce a unique lubricating effect between CPs, facilitating mobility of the CPs once a critical stress is exceeded. [23, 24] Upon bubble shrinking, the CPs aggregates were observed to form a crumpled particle multilayer surrounding the shrinking bubbles (Fig. 3e), before the CPs aggregates finally precipitated once the shrinking bubble vanished (Fig. 3f).

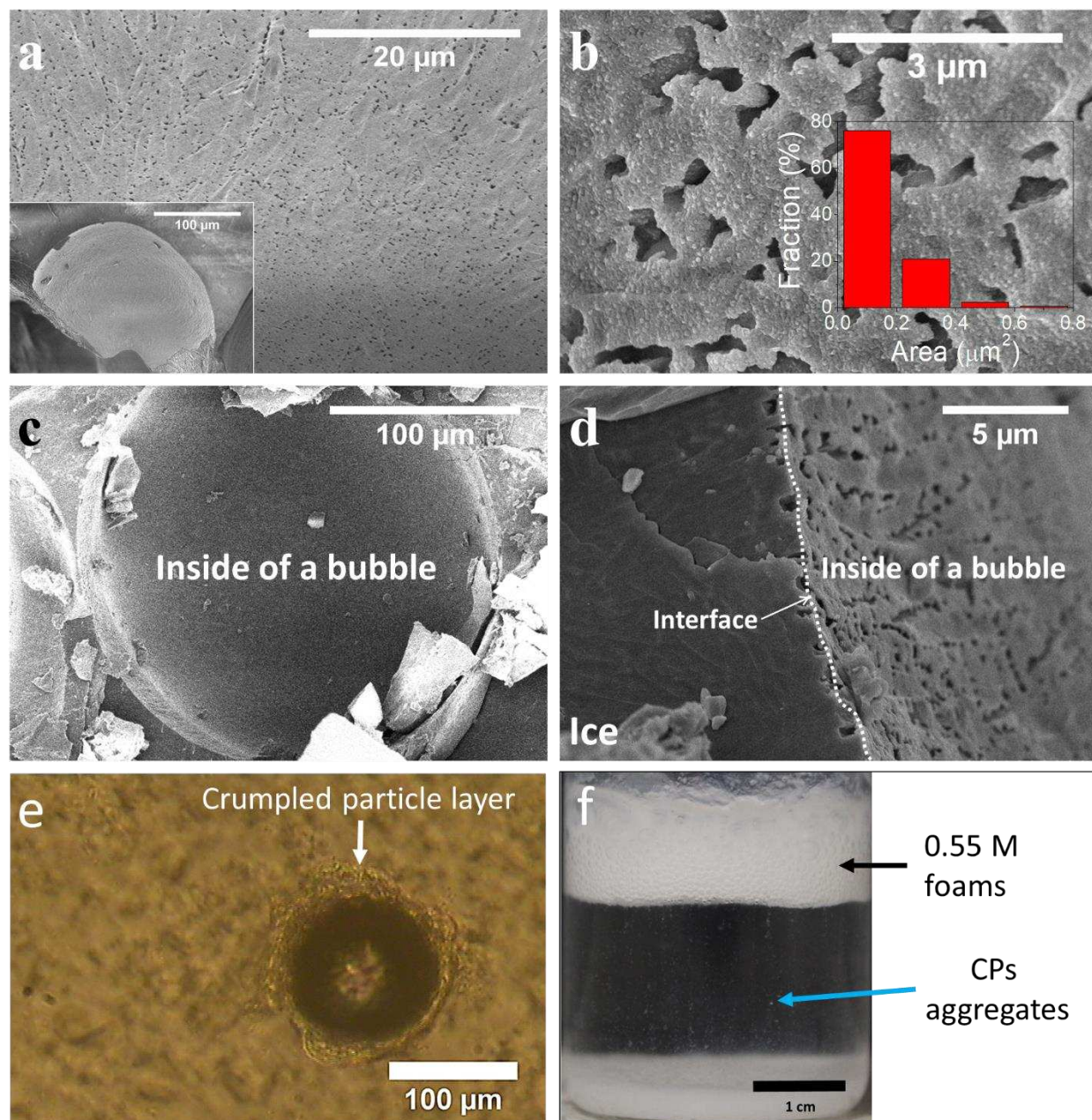


Figure 3. (a) Interfaces surrounding newly-prepared 0.55 M bubbles. (b) Higher magnification image of the 0.55 M bubble-stabilizing particle network in Fig. 3a, the inset shows the pore size distribution and fraction. (c) Low and (d) high magnification Cryo-SEM images showing the internal structure of the 0.55 M bubble-stabilizing film (observed from the inside of 0.55 M bubbles). (e) Crumpled CPs multi-layers surrounding a shrinking 0.55 M bubble. (f) Digital photo showing precipitation of the CPs aggregates from the 0.55 M foam.

Surface expansion of the 0.55 M bubbles were also studied (Fig. 4). As shown in Fig. 4a-c, bubble expanding and shrinking takes place simultaneously. For bubbles being sealed inside a flat-edged capillary tube, the expanding bubbles would be flattened once size of the bubble is greater than the inside thickness (0.5 mm) of the capillary tube, forming a cylinder-like construction (inset of Fig. 4d). Hence, structure of the flattened bubble-stabilizing interface can then be observed using an optical microscope. As shown in Figs. 4d-e, the CPs aggregates are found to be separated by CPs-free interface, which is expected since bubble expanding increases its surface area whilst reducing particle surface coverage. The patchy structure was also confirmed by confocal microscopy analysis by scanning the three-dimensional structure surrounding expanding bubbles (Fig. 4f).

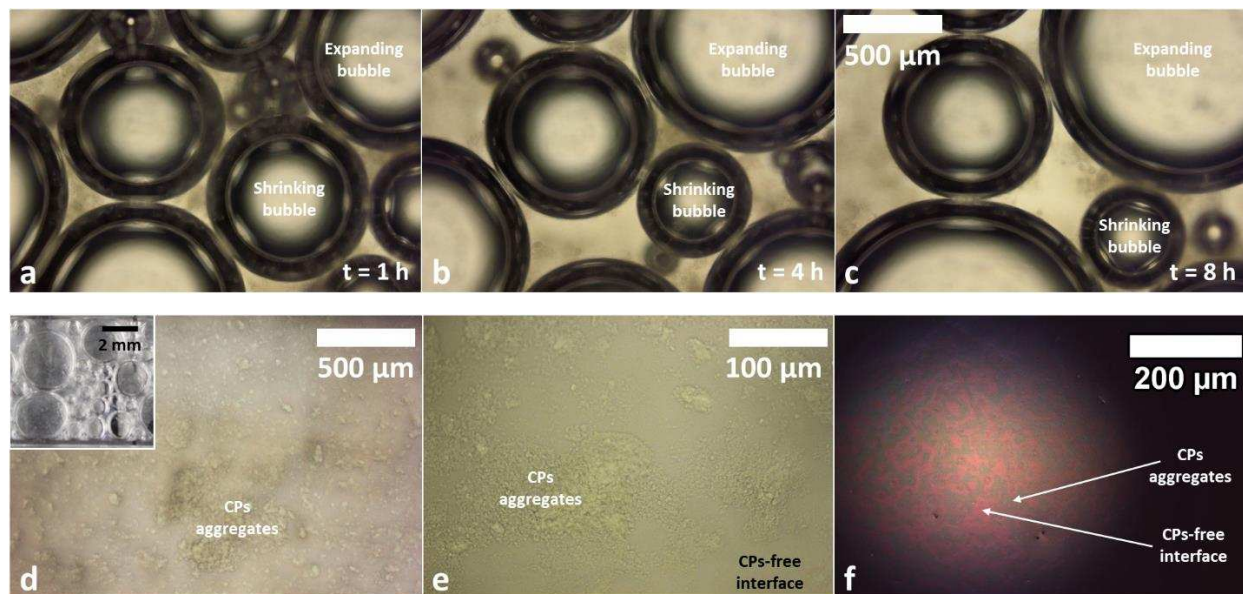


Figure 4. (a-c) Images of 0.55 M coarsening bubbles at various aging time after the foam being prepared. (d) Low and (e) high magnifications images showing structure of the flattened bubble-stabilizing interface, the inset in Fig. 5d shows the flattened 0.55 M bubbles inside a flat-edged capillary tube. (f) Confocal microscopy image showing the three-dimensional structure surrounding an expanding 0.55 M bubble.

3.2 Interfacial behaviour of CPs during accelerated bubble coalescence

Lifetime of the 0.1 M and 0.55 M foams were ~ 16 and ~ 250 hours respectively (Fig. S4). The 0.1 M to 0.55 M transition foaming behavior was studied by generating foams at 0.1 M Na_2SO_4 followed by *in-situ* increasing the bulk electrolyte concentration to 0.55 M, see Scheme S1 in the Supporting Information for more details. Higher concentration electrolyte would diffuse through the thin liquid films between the 0.1 M bubbles (Fig. S3a) and then affect the CPs behavior at the interface. Surprisingly, rapid bubble coalescence was observed for the transition foams, with all the bubbles disappeared within ~ 2 hours (Fig. S4), while the method for transition foam preparation was proven not to affect foam coalescence behavior (Supporting Information). Mechanism of the accelerated bubble coalescence were better understood by studying the interfacial behavior of the CPs using the Cryo-SEM (Fig. 5).

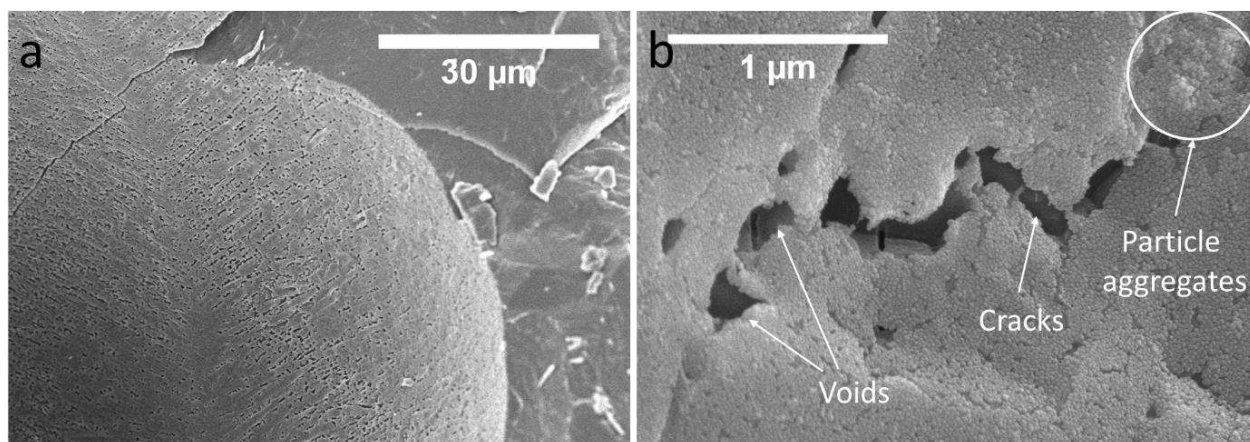


Figure 5. (a) Cryo-SEM image of the interface surrounding a transition bubble, (b) cracks and CPs aggregates being observed in a higher magnification image.

Preparing bubbles in 0.1 M Na_2SO_4 resulted in closely-packed CPs film (Fig. 1a and 1b). Size of the CPs and the silica particle core were measured to be ~ 32.1 nm (Fig. 1d) and ~ 29.5 nm, respectively, suggesting thickness of the PVP shell is ~ 1.3 nm. Hence, it can reasonably assume that distance between the CPs cores is in the range of ~ 1.3 - 2.6 nm at a 0.1 M bubble-stabilizing interface (Fig. S5a and S5b). Whereas patchy structure was observed on the transition bubble-stabilizing interface (10 min after the electrolyte was added), showing an apparent particle surface

coverage of ~ 90% (Fig. 5). Attempts were made to measure the CPs size through high-resolution Cryo-SEM imaging; however, the CPs aggregated and deformed during the transition process (Fig. 5b), significantly interfering with particle size measurement. A higher electrolyte concentration enhances affinity of CPs at the interface,[21] whilst leading to adhesion of interpenetrating PVP chains (Fig. S1b), and hence the likelihood of CPs desorption from the interface would be markedly minimized. Assuming the same amount CPs adsorbing at the interface, reduction of the particle surface coverage indicates decrease of the CPs size, which is calculated to be ~ 30.4 nm. The PVP shell thickness is thus reduced to ~ 0.5 nm due to its poor solubility in 0.55 M electrolyte, while distance between the CPs cores decreases to the range of ~ 0.5-1.0 nm on the transition foam interface (Fig. S5c and S5d).

Decrease of the CPs-CPs distance enhances the attraction potential between the silica particle cores. The interaction potential between silica particles was calculated to be approximately -5 kT at 0.55 M electrolyte, when the separation distance between particles is ~ 1 nm.[25] The negative sign indicates the total interaction potential between particles is attractive. For extreme cases (see Fig. S5d), the potential required to separate the interpenetrating PVP layers is calculated to be ~ 1.3 kT, based on a simplified model we proposed (see the Supporting Information for more details). Hence, in the transition process, the attraction potential between the silica particle cores is able to overcome the adhesion between the interpenetrating PVP layers, forcing the CPs to rearrange and aggregate *in-situ* at the interface. Aggregation of the CPs results in particle-rich (particle aggregates or clusters) and particle-poor (cracks and voids) areas (Fig. 5b), and hence the densely-packed CPs film that originally formed at 0.1 M (Fig. 1a and 1b) would crack in tension. It should be noted that neither particle desorption nor interface expansion can lead to film cracking, as has been proved in Fig. 1d and Fig. 4, respectively. Meanwhile, the osmotic pressure caused by electrolyte concentration difference between the bulk liquid and the foam may accelerate drainage, thinning the film between bubbles. Those cracks and voids (Fig. 5b) become vulnerable spots of the pseudo-solid-like particle films that initially formed at 0.1 M, leading to accelerated bubble coalescence (Fig. S4).

4. CONCLUSION

Preparing multiphase materials (e.g., foams and emulsions) using composite particles (CPs) is extremely versatile as the interface provides an unique platform for particle assembly while different parts of the CPs can bring different functionalities.[4] While CPs are usually prepared via chemical grafting technique,[5, 7, 16-18] few studies consider the interfacial behaviour of CPs produced via physisorptions, an approach which is more applicable for mass production. Furthermore, dynamics of the CPs was usually studied at 2D planar interface using Langmuir Trough, interfacial shear rheometer and BAM, etc., to interpret the underlying mechanism that determines the stability of multiphase materials, whereas behaviour of the CPs at bubble-stabilizing interface (curved interface) during coarsening and coalescence is still poorly understood. [4]

In the current study, high resolution Cryo-SEM was originally used to investigate the behaviour of CPs at the bubble-stabilizing interface during coarsening and coalescence. We found that dynamics of the CPs during bubble coarsening is highly dominated by the behaviour of the polymer layer, while in-situ particle aggregation would lead to accelerated bubble coalescence. The 0.1 M bubble-stabilizing interface buckles in uniaxial compression due to coarsening, with the CPs being observed to desorb from the interface. Although bubble coalescence was inhibited at 0.55 M electrolyte, the CPs rearrange into crumpled particle multi-layers surrounding the shrinking bubbles, due to the adhesion between interpenetrating polymer chains and the unique lubrication effect of the PVP layers. The 0.1 M to 0.55 M transition foaming behaviour and the underlying mechanism were also studied. The interface cracks in tension that driven by *in-situ* CPs aggregation, leading to accelerated bubble coalescence.

Building on the fundamental understanding of the CPs interfacial behaviour will enable the regulation of properties from multiphase materials prepared thereof. The unique core-shell nature of the CPs also enables distinct characteristics of particle-stabilized multiphase systems, such as stimuli-responsiveness or viscoelasticity, to be obtained and finely tuned by simple physico-chemical adjustments of the CPs structure. Further research is planned to optimize the CPs

property to localise particles at the interface with much higher concentrations and adsorption strength, enabling non-equilibrium kinetically trapped stabilised states. This will impart enhanced interfacial and bulk mechanical properties, while offering a unique and material efficient route to structure otherwise all-liquid materials, either as a final product or an intermediate (e.g., via 3D printing).

ASSOCIATED CONTENT

Conflicts of interest

There are no conflicts to declare.

Supporting Information

TEM images of the (a) CPs, and (b) interpenetrating polymer chains between CPs that formed in 0.55 M Na₂SO₄ (Fig. S1); (a) Cryo-SEM image of the freshly prepared 0.1 M bubbles and (b) bubble size distribution measured by ImageJ software (Fig. S2); Optical microscope images of newly-prepared (a) 0.1 M bubbles separated by thin liquid films and (b) 0.55 M bubbles separated by thick liquid films (Fig. S3); (a) Foam height as a function of aging time for sample 1, 2, and 3 (sample 1: the transition foam, sample 2: the 0.1 M foam, sample 3: the 0.55 M foam). (b) Image showing remained foams of sample 1, 2, and 3 after 2h the foams had been prepared, height of the glass vial = 9 cm (Fig. S4); Schematic of distance between the CPs cores at 0.1 M (a, b) and 0.55 M (c, d) bubble-stabilizing interfaces (Fig. S5).

Corresponding Authors

K. Y. – Email: victoryu66@ujs.edu.cn

B. L. – Email: binli@ujs.edu.cn

ACKNOWLEDGMENTS

K.Y. would like to thank the National Natural Science Foundation of China (52206198, 52206199, 52076105), Natural Science Foundation of Jiangsu Province (No. BK20210759), China

Postdoctoral Science Foundation (No. 2020M681506), Key Laboratory of Modern Agricultural Equipment and Technology (Jiangsu University), Ministry of Education (MAET202115), Jiangsu Province and Education Ministry Co-sponsored Synergistic Innovation Center of Modern Agricultural Equipment (XTCX2028), Senior Talent Foundation of Jiangsu University (19JDG029), Jiangsu Agricultural Science and Technology Innovation Fund (CX(21)3079) for supporting this research.

References

- [1] Y. Liu, B.P. Binks, *J Colloid Interf Sci* 583 (2021) 522.
- [2] Y. Liu, B.P. Binks, *J Colloid Interf Sci* 594 (2021) 204.
- [3] K.D. Guo, P. Wei, Y.H. Xie, X.L. Huang, *Chem Commun* 58 (2022) 4723.
- [4] K. Yu, B. Li, H.G. Zhang, Z.T. Wang, W. Zhang, D.B. Wang, H.J. Xu, D. Harbottle, J.F. Wang, J.M. Pan, *Chem Eng J* 416 (2021) 129121.
- [5] K. Yu, H.G. Zhang, S. Tangparitkul, J.T. Jiang, C. Hodges, D. Harbottle, *J Colloid Interf Sci* 613 (2022) 827.
- [6] S.M. Kirby, S.L. Anna, L.M. Walker, *Soft Matter* 14 (2018) 112.
- [7] F. Grillo, M.A. Fernandez-Rodriguez, M.N. Antonopoulou, D. Gerber, L. Isa, *Nature* 582 (2020) 219.
- [8] D. Harbottle, Q. Chen, K. Moorthy, L.X. Wang, S.M. Xu, Q.X. Liu, J. Sjoblom, Z.H. Xu, *Langmuir* 30 (2014) 6730.
- [9] A. Maestro, O.S. Deshmukh, F. Mugele, D. Langevin, *Langmuir* 31 (2015) 6289.
- [10] M. Rey, M.A. Fernandez-Rodriguez, M. Karg, L. Isa, N. Vogel, *Accounts Chem Res* 53 (2020) 414.
- [11] S.N. Tao, H. Jiang, R.J. Wang, C. Yang, Y.X. Li, T. Ngai, *Chem Commun* 56 (2020) 14011.
- [12] Y. Sheng, K. Lin, P.B. Binks, T. Ngai, *J Colloid Interf Sci* 579 (2020) 628.
- [13] K. Heise, E. Kontturi, Y. Allahverdiyeva, T. Tammelin, M.B. Linder, Nonappa, O. Ikkala, *Adv Mater* 33 (2021).
- [14] S. Eyley, W. Thielemans, *Nanoscale* 6 (2014) 7764.
- [15] P. Rattanadom, B.J. Ben Shiau, J.H. Harwell, U. Suriyapraphadilok, A. Charoensaeng, *J Petrol Sci Eng* 209 (2022).
- [16] P.J. Beltramo, M. Gupta, A. Aliche, I. Liascukiene, D.Z. Gunes, C.N. Baroud, J. Vermant, *P Natl Acad Sci USA* 114 (2017) 10373.
- [17] K. Yu, H.G. Zhang, Z.T. Wang, W. Zhang, H.J. Xu, Y.Y. Chen, H.S. Li, B. Li, J.F. Wang, *Journal of Molecular Liquids* 352 (2022).
- [18] Z.F. Li, D. Harbottle, E. Pensini, T. Ngai, W. Richtering, Z.H. Xu, *Langmuir* 31 (2015) 6282.
- [19] K. Yu, B. Li, Z.T. Wang, W. Zhang, D.B. Wang, H.J. Xu, J.F. Wang, D. Harbottle, *Ind Eng Chem Res* 59 (2020) 7495.
- [20] A.L. Fameau, S. Fujii, *Curr Opin Colloid In* 50 (2020).

- [21] K. Yu, H. Zhang, C. Hodges, S. Biggs, Z. Xu, O.J. Cayre, D. Harbottle, *Langmuir* 33 (2017) 6528.
- [22] A. Mikkelsen, Z. Rozynek, *Acs Appl Mater Inter* 11 (2019) 29396.
- [23] K. Yu, H.G. Zhang, S. Biggs, Z.H. Xu, O.J. Cayre, D. Harbottle, *J Colloid Interf Sci* 527 (2018) 346.
- [24] K. Yu, C. Hodges, S. Biggs, O.J. Cayre, D. Harbottle, *Ind Eng Chem Res* 57 (2018) 2131.
- [25] H. Zhang, K. Yu, O.J. Cayre, D. Harbottle, *Langmuir* 32 (2016) 13472.